ELSEVIER

Journal of Alloys and Compounds 404–406 (2005) 752–756

Journal of ALLOYS AND COMPOUNDS

www.elsevier.com/locate/jallcom

Thermal decomposition of $Mg(AlH_4)_2$ studied by in situ synchrotron X-ray diffraction

A. Fossdal[a,*], H.W. Brinks[a], M. Fichtner[b], B.C. Hauback[a]

[a] *Department of Physics, Institute for Energy Technology, P.O. Box 40, NO-2027 Kjeller, Norway*
[b] *Karlsruhe Research Center, Institute of Nanotechnology, P.O. Box 3640, D-76021 Karlsruhe, Germany*

Received 6 September 2004; received in revised form 6 December 2004; accepted 14 December 2004
Available online 14 July 2005

Abstract

The thermal decomposition of $Mg(AlH_4)_2$ was studied by in situ synchrotron X-ray diffraction. The reaction proceeds in two steps. The first reaction step involves decomposition of magnesium alanate to magnesium hydride and the solid solution $Al_{1-x/2}Mg_{x/2}$: $(1 - x/2)Mg(AlH_4)_2 \rightarrow (1 - (3/2)x)MgH_2 + 2Al_{1-x/2}Mg_{x/2} + (3 + (3/2)x)H_2$. No evidence of intermediate phases was found. The second step proved to be more complex. For simplicity this step can be written as: $(1 - (3/2)x)MgH_2 + 2Al_{1-x/2}Mg_{x/2} \rightarrow Al_xMg_y + (1 - (3/2)x)H_2$, where Al_xMg_y represents either two cubic Al–Mg solid solution phases or the ordered β-Al_3Mg_2 phase.

Keywords: Hydrogen storage materials; Crystal structure; Neutron diffraction; Synchrotron radiation; Alanates

1. Introduction

Magnesium alanate, $Mg(AlH_4)_2$, an alkaline earth alanate, is a potential hydrogen storage candidate with a hydrogen content of 9.3 wt.%. $Mg(AlH_4)_2$ is thought to decompose in a two-step reaction, however the exact mechanism of the two reactions is still somewhat unclear. According to Wiberg and Bauer [1], Dymova et al. [2] and Fichtner et al. [3], the first reaction proceeds as

$$Mg(AlH_4)_2 \rightarrow MgH_2 + 2Al + 3H_2 \quad (1)$$

Reaction (1) has been found to occur at temperatures of 135–163 °C [1–3]. In a later paper, Dymova et al. [4] suggest that reaction (1) in fact is the sum of two temperature-separated reactions involving an intermediate phase, $MgAlH_5$:

$$Mg(AlH_4)_2 \rightarrow MgAlH_5 + Al + 1.5H_2 \quad (120–155\,^\circ C) \quad (2)$$

$$MgAlH_5 + Al \rightarrow MgH_2 + 2Al + 1.5H_2 \quad (210–255\,^\circ C) \quad (3)$$

$MgAlH_5$ has not been observed by X-ray diffraction, but thermovolumetric [4] and TGA-MS [5] analyses show features compatible with several steps in the first decomposition reaction.

Two alternative reaction paths have also been suggested for the second reaction step. Dymova et al. [2,4], observed direct reaction between magnesium hydride and aluminium to one (380–420 °C) or two (270–310 °C) Al–Mg alloy phases, whereas Fichtner et al. [5,6] found that alloy formation only occurred subsequent to decomposition of magnesium hydride to the constituent elements at around 300 °C.

In the present study, the thermal decomposition of magnesium alanate under vacuum has been investigated by in situ synchrotron powder X-ray diffraction. Particular emphasis has been put on resolving whether or not $MgAlH_5$ or any other intermediate phase participates in the first step of decomposition.

2. Experimental

$Mg(AlH_4)_2$ was synthesized via a metathesis reaction of $NaAlH_4$ and $MgCl_2$ in diethyl ether, with subsequent

* Corresponding author. Tel.: +47 63 80 62 73; fax: +47 63 81 09 20.
E-mail address: anita.fossdal@ife.no (A. Fossdal).

0925-8388/$ – see front matter © 2005 Elsevier B.V. All rights reserved.
doi:10.1016/j.jallcom.2004.12.169

purification and solvent removal. The procedure is described in detail elsewhere [7]. Due to the preparation route, a NaCl impurity is present in the resulting white powder. NaCl was included in the Rietveld refinements (space group $Fm\bar{3}m$, $a = 5.6394(4)$ Å at 295 K), and the content of NaCl was found to be approximately 4 wt.%. In addition, trace amounts of Al (<0.3 wt.%) were present in the powder.

Time-resolved powder X-ray diffraction (PXD) data were collected at the Swiss-Norwegian beam line (station BM01A) at the European Synchrotron Radiation Facility (ESRF) in Grenoble, France. The sample was contained in a 0.5 mm boron–silica–glass capillary, kept in place by a glass rod, and mounted in a Swagelok fitting. The capillary was then evacuated and kept under dynamic vacuum for the duration of the experiment. A hot-air blower was used to heat the capillary at constant heating rates of 2, 5 or 10 K/min or to constant temperatures (164–183 °C). Two-dimensional powder diffraction data were collected using an imaging plate system (MAR345) with an exposure time of 30 s. The capillary was rotated 10° during the exposure. Data were collected every second minute, owing to the required read and erase time of the image plate. The wavelength was 0.71000 Å (2 and 10 K/min) or 0.70000 Å (5 K/min). The two-dimensional data were converted to one-dimensional powder diffraction patterns with the program Fit2D [8,9]. Data were collected in the range 10–33.5° and were rebinned with a step size of 0.015°. Temperature calibration was performed by measuring the melting temperature of six compounds with melting points in the range 125–327.5 °C. In addition, measurements were performed on a Ni sample every 25 °C between room temperature and 450 °C and the cell parameter and thermal expansion were compared with literature values. Combining these two types of measurements a relationship was found between the set point temperature and the actual temperature value.

Rietveld refinements were carried out with the program Fullprof (Version 2.50) [10]. The X-ray form factor coefficients were taken from the Fullprof library. Pseudo-Voigt profile parameters were used and background modelling was performed by linear interpolation between manually selected points.

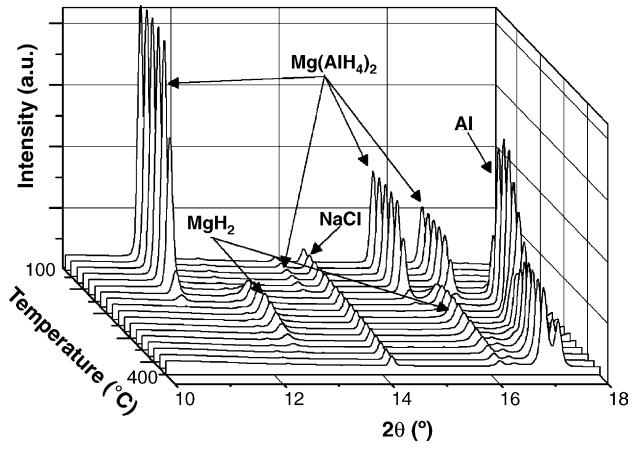

Fig. 1. In situ PXD data collected during heating in vacuum in the temperature range 100–400 °C at a heating rate of 10 K/min.

3. Results and discussion

Time-resolved in situ PXD data collected with a heating rate of 10 K/min between 100 and 400 °C are shown in Fig. 1. The experiments with lower heating rates (2 and 5 K/min) followed the same course of reaction as for 10 K/min. No intermediate phases were observed during the first decomposition reaction at heating rates of 2, 5 or 10 K/min, thus decomposition of $Mg(AlH_4)_2$ proceeds according to the reaction

$$\left(1 - \frac{x}{2}\right) Mg(AlH_4)_2 \rightarrow \left(1 - \frac{3}{2}x\right) MgH_2 + 2\,\alpha + \left(3 + \frac{3}{2}x\right) H_2 \quad (4)$$

where α is a solid solution of Mg in Al of composition $Al_{1-x/2}Mg_{x/2}$. According to the Al–Mg phase diagram [11] the solid solubility of Mg in Al increases from 2 at.% Mg ($x = 0.04$) at 150 °C to 18.6 at.% Mg ($x = 0.372$) at the eutectic temperature (450 °C). Dissolution of Mg in Al causes an increase in the unit cell parameter of Al [12]. Formation of α rather than pure Al in (4) is thus supported by the rapid increase in the unit-cell parameter of α beginning at 150 °C at 2 K/min (Fig. 2), coinciding with the onset of decomposition of $Mg(AlH_4)_2$ at this heating rate (Fig. 3). At temperatures above 180 °C, where decomposition approaches completion, the slope of the α cell parameter versus temperature decreases again, but is still higher than it was below 150 °C. As the thermal expansion should be approximately constant with temperature, this is in accordance with the increased solubility of Mg in α with increasing temperature. Experiments at constant temperature (164–183 °C) show that the first decomposition reaction is rather slow, traces of $Mg(AlH_4)_2$ remaining even after 1 h of annealing at these temperatures. No evidence could be found of intermediate phases during isothermal decomposition, consistent with the experiments conducted under dynamic temperature conditions. The time resolution of these in situ experiments should be more than sufficient to observe any crystalline intermediate phases participating in the decomposition of $Mg(AlH_4)_2$ to α-phase and MgH_2. The cell parameters of $Mg(AlH_4)_2$ are given in Fig. 2 as a function of temperature at a heating rate of 2 K/min. Prior to onset of decomposition at approximately 150 °C, the decrease in a and increase in c is in accordance with previous results [13]. The rate of change increases for both cell parameters as the decomposition proceeds. As an example, $\Delta c/c$ is 0.003% K^{-1} at 140–160 °C, rising to 0.03% K^{-1} at 200–220 °C. Note that the cell parameter of NaCl (insert in Fig. 2), which can be seen as an internal standard, increases linearly

with temperature, showing that the unusual behavior of the $Mg(AlH_4)_2$ and α cell parameters is not an effect of temperature changes in the sample during decomposition. Similarly, large shifts in the $Mg(AlH_4)_2$ cell parameters during decomposition are also seen for 5 and 10 K/min, however the magnitude of the change decreases with increasing heating rate. Introduction of point defects on H sites during decomposition is unlikely to be the cause of the observed changes in the cell parameters as Al and Mg have fixed oxidation states of +3 and +2, respectively, in this case. Instead, it is reasonable to assume that increased tilting and/or distortion in the Al–H and Mg–H coordination polyhedra is occurring. Neutron diffraction data would however be needed to confirm this. In Fig. 3 the content of $Mg(AlH_4)_2$ (wt.%) is shown as a function of temperature and heating rate. The smooth decrease in $Mg(AlH_4)_2$ content during heating is accompanied by the emergence and subsequent increase in the content of α-phase and MgH_2 in a molar ratio of 2:1. NaCl remains inert throughout all decomposition experiments. The α:MgH_2 ratio increases slightly with increasing temperature, as more Mg from MgH_2 is dissolved into the α-phase in accordance with the Al–Mg phase diagram [11] and the α cell parameter (Fig. 2). The fact that the α:MgH_2 ratio is in accordance with reaction (4) is indirect proof that no amorphous intermediate phases are present, hence the direct reaction route is confirmed. The temperatures of onset and end of the first decomposition reaction are given as a function of heating rate in Fig. 4, and are seen to increase linearly with heating rate. According to Gibbs phase rule, reaction (4) corresponds to an invariant point, i.e. occurs at one temperature rather than in a temperature range. The fact that extrapolation of the onset and end temperatures of the reaction down to 0 K/min does not give coinciding temperature values hence reflects the sluggish nature of reaction (4) rather than a state of equilibrium. It must be noted that the reaction temperatures have been observed to vary in the order of 5–20 °C between experiments performed under nominally identical conditions. The cause of this variation is not clear, but as the reaction is characterized by slow kinetics, even small differences in e.g. temperature gradients during heating of the sample may potentially influence the nucleation and growth of the decomposition products. Differences in experimental conditions are also thought to be the reason for the wider temperature region of decomposition as compared to previous studies [1–3].

The second decomposition step proved less predictable in terms of decomposition products. According to the Al–Mg phase diagram [11], a 2:1 Al:Mg mixture should yield a two-phase mixture of an Al-rich fcc Al–Mg solid solution (α) and an ordered fcc phase of approximate composition Al_3Mg_2 (β). β-Al_3Mg_2 (space group $Fd\bar{3}m$) has approximately 1168 atoms in the unit cell and the unit-cell parameter $a = 28.239(1)$ Å at room temperature [14]. The two-phase mixture of α and β was found in a previous study [3], where $Mg(AlH_4)_2$ was treated in a N_2 atmosphere at 400 °C for 30 min in an Al_2O_3 boat. Zhang et al. [15] have however

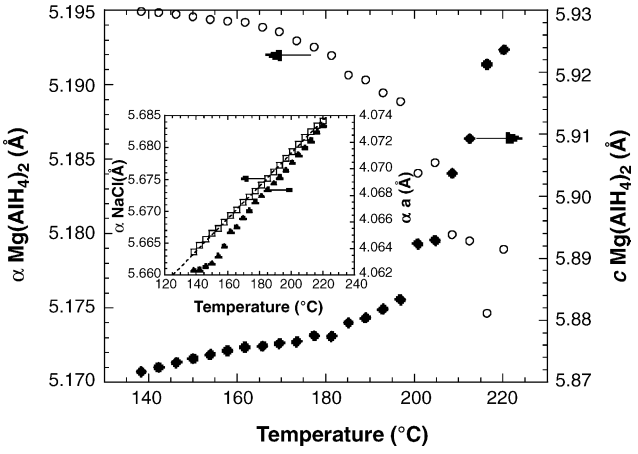

Fig. 2. Temperature evolution of the unit-cell parameters *a* (circles) and *c* (filled diamonds) of $Mg(AlH_4)_2$ at a heating rate of 2 K/min. The corresponding unit-cell parameter of the α solid solution (filled triangles) and the impurity phase NaCl (open squares) are shown as an insert.

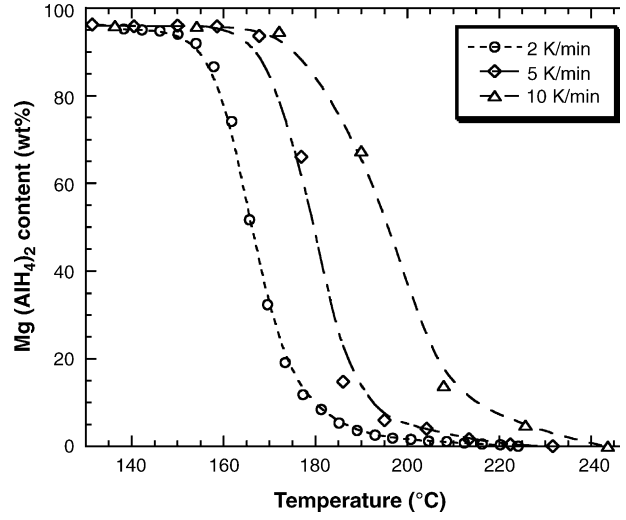

Fig. 3. Content of $Mg(AlH_4)_2$ (wt.%) during the first decomposition reaction as a function of temperature and heating rate.

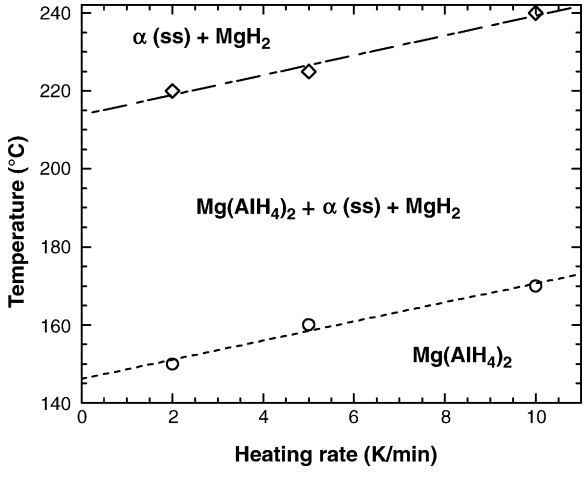

Fig. 4. Temperatures of onset and end of the decomposition of $Mg(AlH_4)_2$ (first decomposition reaction) as a function of heating rate.

shown that although β-Al_3Mg_2 is the thermodynamically stable phase in this compositional region, a supersaturated, metastable fcc Al–Mg solid solution phase may coexist with the α-phase at low temperatures. By elevating the temperature, cation diffusion rates are increased and the metastable Al–Mg phase may transform to the stable, ordered β-Al_3Mg_2 phase. In fact, three different sets of reaction products were observed for the reaction of MgH_2 and Al, examples of which are shown in Fig. 5. It must be noted that the differing reaction products cannot be explained by differences in sample preparation or aging of the material, as all experiments were performed with the same powder and experiments performed in rapid succession could yield completely different results. Also, as all sample preparation was performed under inert atmosphere, exposure to air prior to the experiments is highly unlikely. In the first set of reaction products (Fig. 5a), observed for heating rates of 2 and 5 K/min, the α phase coexists with an unknown phase (for simplicity termed X). The X phase shows two severely broadened peaks (or clusters of peaks), located to the left of the Al (2 0 0) and (2 2 0) reflections. MgH_2 is consumed as the amount of X phase increases. The amount of α-phase (Al-rich) is also seen to decrease at high temperatures. It is likely that the X phase is an impurity phase formed by reaction of Mg and Al with oxygen from air, which could occur in case of a small leakage in the capillary setup. The fact that melting was not observed above the eutectic point in the Al–Mg system (450 °C) [11] gives support to the presumption that the composition has been shifted out of the Al–Mg binary. In the second set of reaction products (Fig. 5b), observed for heating rates of 2 and 10 K/min, the metastable Al–Mg solid solution is seen in addition to the α and X phases. At 2 K/min, the metastable Al–Mg phase was initially formed at approximately 260 °C, whereas the X-phase was first observed at 290 °C. Increasing the heating rate to 10 K/min elevated these temperatures by ∼50 °C. The amount of X-phase increases continuously with temperature, whereas the amount of the metastable phase shows an initial increase before decreasing again at higher temperatures. The amount of α-phase is inversely related to the amount of metastable Al–Mg solid solution. Again, this is an indication that the impurity phase (X) is Mg-rich and can consume the amount of Mg that exceeds the solubility limit in the α-phase, i.e. most of the Mg present in the metastable solid solution. The Al from the metastable phase returns to the α solid solution. In the third case, observed for heating rates of 5 and 10 K/min, neither the metastable Al–Mg solid solution nor the X-phase are seen (Fig. 5c). Instead, the α phase reacts with MgH_2 to form the ordered β-Al_3Mg_2 phase with little or no α phase remaining. As the Al:Mg ratio in $Mg(AlH_4)_2$ is 2:1 rather than 3:2, the β-Al_3Mg_2 phase is expected to have variable composition. The cell parameter of the β-Al_3Mg_2 phase varied linearly with temperature. Extrapolation of the cell parameter to room temperature gave $a = 28.179(2)$ Å, which is significantly lower than previously reported for β-Al_3Mg_2 [14]. By analogy with dissolution of Mg in Al [12], an increase in the Al-content relative to the 3:2 composition should decrease the unit-cell parameter. Variable composition in the β-phase was also observed by Samson [14], who obtained single-phase material in the investigated compositional range $Al_{2.96–3.17}Mg_2$.

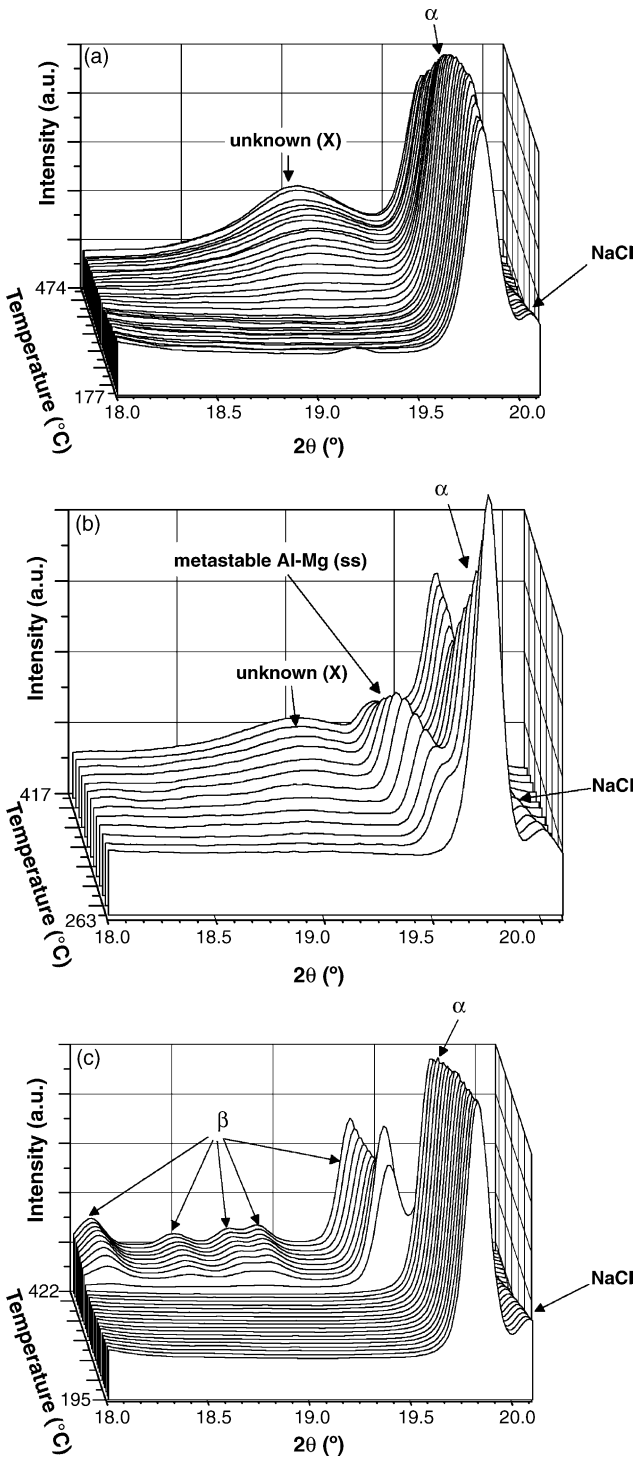

Fig. 5. In situ PXD data during heating in vacuum showing phase evolution during the reaction of MgH_2 and α (second decomposition reaction): (a) phase composition α (ss) and the impurity phase X; (b) phase composition α (ss), metastable Al(Mg) (ss) and the impurity phase X; (c) formation of β-Al_3Mg_2 (ss) at high temperatures.

As seen above, no correlation could be found between the applied heating rate and the resulting decomposition products of the second decomposition step. Usually, metastable phases appear upon rapid heating. All heating rates in this work can be considered to be high, hence metastable phases are expected as an alternative to the thermodynamically stable decomposition products. The absence of a second Al–Mg phase in Fig. 5a is however more difficult to explain. Initial formation of the thermodynamically stable β-Al_3Mg_2 phase in other experiments could occur as high as 350 °C. Here, the X-phase is formed at ∼330 °C, which shifts the sample composition out of the Al–Mg binary. It is therefore likely that had the X-phase impurity not been formed, the β-Al_3Mg_2-phase would have appeared at higher temperatures, as seen in Fig. 5c. Thus, the thermodynamically stable second decomposition step can be written as

$$\left(1-\frac{3}{2}x\right)\mathrm{MgH_2} + 2\,\alpha \rightarrow A\,\alpha + B\,\beta - \mathrm{Al}_{3+y}\mathrm{Mg}_2 + \left(1-\frac{3}{2}x\right)\mathrm{H_2} \quad (5)$$

where $A = \frac{(2-x)(1-y)}{4-x(5+y)}$, $B = \frac{x(4-(3/2)x)-2}{x(5+y)-4}$ and α is assumed to be of constant composition $\mathrm{Al}_{1-x/2}\mathrm{Mg}_{x/2}$

The alternative, metastable reaction

$$\left(1-\frac{3}{2}x\right)\mathrm{MgH_2} + 2\,\alpha \rightarrow C\,\alpha + D\mathrm{Al}_{1-z}\mathrm{Mg}_z(\mathrm{ss}) + \left(1-\frac{3}{2}x\right)\mathrm{H_2} \quad (6)$$

where $C = \frac{2+x(3z-1)-6z}{x-2z}$, $D = \frac{x(4-(3/2)x)-z}{x-2z}$ and α is again assumed to be of constant composition $\mathrm{Al}_{1-x/2}\mathrm{Mg}_{x/2}$, is also likely to occur under dynamic conditions. The metastable Al–Mg phase is written as $\mathrm{Al}_{1-z}\mathrm{Mg}_z$ (ss) and is richer in Mg than the α-phase, hence $z > x/2$. The onset of reaction (5) was observed at 260–350 °C, with complete consumption of MgH_2 at 390–405 °C. Reaction (6) was seen to start at 260–290 °C and was completed at 390–415 °C.

Acknowledgements

The work has received financial support from project "Hydrogen Storage Systems for Automotive Applications - STORHY" (contract no. 502667) under the FP6-2002-Energy program in the European Commission. The assistance by the project team at the Swiss-Norwegian Beam Line, ESRF is gratefully acknowledged.

References

[1] E. Wiberg, R. Bauer, Z. Naturforsch. 7b (1952) 131.
[2] T.N. Dymova, V.N. Konoplev, A.S. Sizareva, D.P. Aleksandrov, Russ. J. Coord. Chem. 25 (1999) 312.
[3] M. Fichtner, O. Fuhr, O. Kircher, J. Alloys Compd. 356/357 (2003) 418.
[4] T.N. Dymova, N.N. Mal'tseva, V.N. Konoplev, A.I. Golovanova, D.P. Aleksandrov, A.S. Sizareva, Russ. J. Coord. Chem. 29 (2003) 385.
[5] M. Fichtner, J. Engel, O. Kircher, O. Rubner, Mater Sci. Eng. B 108 (2004) 42.
[6] M. Fichtner, J. Engel, O. Fuhr, A. Glöss, O. Rubner, R. Ahlrichs, Inorg. Chem. 42 (2003) 7060.
[7] M. Fichtner, O. Fuhr, J. Alloys Compd. 345 (2002) 286.
[8] A.P. Hammersley, Internal Report ESRF-97-HA02T, 1997.
[9] A.P. Hammersley, Internal Report ESRF-98-HA01T, 1998.
[10] J. Rodríguez-Carvajal, Physica B 192 (1993) 55.
[11] J.L. Murray, Bull. Alloy Phase Diagrams 3 (1982) 60.
[12] G. Siebel, H. Vosskühler, Z. Metallkd. 31 (1939) 359.
[13] A. Fossdal, H.W. Brinks, M. Fichtner, B.C. Hauback, J. Alloys Compd. 387 (2005) 47.
[14] S. Samson, Acta Crystallogr. 19 (1965) 401.
[15] D.L. Zhang, T.B. Massalski, M.R. Paruchuri, Metall. Mater. Trans. A 25 (1994) 73.